Nanoparticle-Free Single Molecule Anti-Stokes Raman Spectroscopy

Lynn Peyser-Capadona,* Jie Zheng, Jose I. González, Tae-Hee Lee,† Sandeep A. Patel, and Robert M. Dickson‡

School of Chemistry and Biochemistry, Georgia Institute of Technology Atlanta, Georgia 30332-0400, USA

(Received 18 August 2004; published 9 February 2005; corrected 30 March 2005)

In the absence of large, plasmon-supporting nanoparticles, biocompatible dendrimer- and peptide-encapsulated few-atom Ag nanoclusters produce scaffold-specific single molecule (SM) Stokes and anti-Stokes Raman scattering. The strong SM vibrational signatures are enhanced by the Ag_n transitions in nanoparticle-free samples and cannot arise from plasmon enhancement. Characteristic SM-Raman intermittency is observed, with antibunching of the underlying Ag_n emission directly confirming the SM nature of the emissive species.

DOI: 10.1103/PhysRevLett.94.058301 PACS numbers: 82.37.Vb, 33.20.Fb, 36.40.Vz, 87.83.+a

Ordinarily exceedingly weak, Raman spectroscopy cross sections can be greatly enhanced when near (40–100)-nm Ag and Au nanoparticle (NP) surfaces such that they even enable facile single molecule observation [1–3]. While single molecule Raman (SM-Raman) spectroscopy is currently the only tool capable of combining chemical information with single molecule sensitivity, the enhancement mechanism remains enigmatic, thereby limiting application. SM-Raman cross sections are only thought to become comparable to those of fluorescence through a combination of chemical/charge transfer interactions combined with large metal NP-assisted plasmon enhancement of the incident electromagnetic field [1–5]. Chemical processes mix energy levels to produce new electronic states in resonance with the laser excitation, but are thought to yield only a small contribution ($\sim 10^3$) to the overall enhancement. The primary effect is thought to arise from extreme plasmon-assisted field enhancements at ill-defined ''hot spots'' [3,6]. While still under debate, the largest such enhancements should occur at NP junctions, a prediction that largely correlates with experimental evidence [7,8]. However, even the most advantageous calculated enhancements ($\sim 10^{11}$) [9,10] typically fall orders of magnitude short of those observed in NP-based SM-surface enhanced Raman spectroscopy (SM-SERS) experiments, which exhibit 10–100 times higher sensitivity than SM fluorescence. Additionally, the NP Rayleigh spectrum (corresponding to plasmon enhancement) was shown to be independent of the spectral dependence that yields Raman enhancement [3], questioning the role of the plasmon in SM-Raman. Very recently, the strong, broad nonresonant background and blinking signals were even shown to be present without added analyte and seem to arise solely from the large metal NP itself [11,12].

Well known at low temperature, strong luminescence has been reported from small ($n \leq 8$ atom) silver nanoclusters (NCs) [13], and more recently from similar Ag_n NCs on thin silver-oxide films [14] and encapsulated in dendrimer hosts at room temperature [15]. The absorption cross sections of these room temperature, few-atom NCs were $\sim 10^{-14}$ cm^2, or $\sim$100 times stronger than those of the best organic fluorophores, and therefore easily observable on the single molecule level. The similar excitation and emission spectra and comparable emissive lifetimes suggest that these NCs are likely a contributing factor to the omnipresent, strong nonresonant background characteristic of SERS experiments [1,11,12].

With very high polarizibilities, these strongly absorbing few-atom metal NCs should strongly interact with analytes in a charge-transfer mechanism to enhance Raman signals. Here we demonstrate that large metal NPs are actually unnecessary to produce SM-Raman signals, with enhancement arising solely from coupling with the strong optical transitions of few-atom Ag NCs. With scaffold-specific Raman scattering, biocompatibility, and even SM–anti-Stokes Raman being observed, these sub-nm Ag NCs open revealing windows into how SM-Raman signals occur.

Small (2–8 atom) Ag NCs were produced within both G4-OH and G2-OH PAMAM [fourth- and second-generation OH-terminated poly(amidoamine)] dendrimers [15] and short amine-rich peptides known to interact with metal ions (peptide sequence: AHHAHHAAD [16]). Exceedingly strong, multicolored single molecule fluorescence is observed from the distribution of small silver NCs with excitation spectra for all NCs peaking at $\sim$475 nm [17]. Any large NPs that may have been produced are removed through centrifugation (20 800 g) before study. No plasmon absorption ($\sim$400 nm) is seen and no features from the sample scatter light when observed with dark-field microscopy, indicating the complete absence of large NPs in the sample. Although the strongly emissive species are 2–8 atom nanoclusters as confirmed by mass spectrometry [15], to provide an additional upper limit on NC sizes we synthesized nearly monodisperse (as determined by transmission electron microscopy) 4-nm diameter Ag NPs in PAMAM [18] and thiol-encapsulated 1.8-nm Au NPs, both of which are clearly observed with dark-field microscopy and can be readily removed from solution by

centrifugation (not shown). Consequently, any emissive feature observed that does not correlate with dark-field scattering must be smaller than 1.8 nm and should correspond to our 2–8 atom NCs if the emission is similar to that previously reported [14,15,17]. Simultaneous dark-field microscopy, wide-field fluorescence, and Raman spectra of features within the same field of view were collected on a high-sensitivity charge-coupled device through an imaging monochromator on an inverted microscope with either a mirror (for imaging) or 600 l/mm grating in the emission path. Raman spectra were collected upon Ar^+ laser excitation in an epifluorescent configuration with dried and solvated samples producing indistinguishable results. The uncorrelated dark-field and single molecule fluorescence images of the same field of view directly demonstrate that the strong peptide- [Figs. 1(a) and 1(b)] and dendrimer-encapsulated [Figs. 1(d) and 1(e)] Ag_n NC emission does not arise from NPs, but instead only from these few-atom, sub-nm Ag NCs. Surprisingly, when excited with narrow band laser illumination, Raman scattering is observed from both samples at the single molecule level with unique scaffold-specific spectra [Figs. 1(c) and 1(f)] on top of the Ag_n fluorescence. Of note is that the spectra are neither from highly polarizable dyes, nor do they result from interactions with large plasmon-supporting metal NPs, but are unique signatures of the unconjugated encapsulating scaffold.

Often considered evidence of single molecule behavior, emission intermittency in both the fluorescence and Raman is readily observed. Such stochastic intermittency will disappear into noise at the level of even several emitters within a given probe volume. The Raman spectra in Figs. 1 and 2 suggest that the scaffold Raman spectrum is measured on top of the strong Ag_n fluorescence. Because individual molecule Raman spectra are known to shift with dynamic relative intensities, the sum of 100 single PAMAM Raman spectra was compared to the summed spectra from 100 peptide-encapsulated Ag NCs, thus accounting for any spectral shifts arising from environmental differences. Clearly the broad fluorescence background is similar [Fig. 2(a)], but the sharp peaks are unique to each scaffold [Figs. 2(b) and 2(c)]. As broad NC fluorescence is unchanged and only the scaffold differs, the background arises from Ag_n fluorescence [14,15,17] while the SM-Raman is characteristic of the scaffold. In fact, our single dendrimer Raman spectra are consistent with the recently reported ordinary bulk PAMAM Raman spectrum [19], with different relative intensities due to chemical interactions with the NC.

Using frequency doubled Ti:sapphire laser excitation (890 nm center frequency, 84 MHz, ~200 fs) at 445 nm (10-nm bandwidth), we probed the wavelength dependent lifetimes of the peptide- and PAMAM-encapsulated NC emission. Emitted light was diverted to a multichannel plate photomultiplier tube at the side port of the monochromator, which, with time correlated single photon counting electronics (Becker-Hickel SPC-630), yields de-

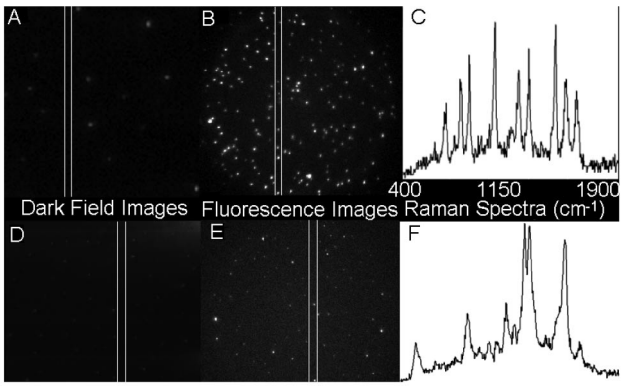

FIG. 1. (a) Dark-field and (b) Stokes-shifted emission images from individual peptide-encapsulated 2–8 atom Ag NCs within the same field of view. (c) Emission spectrum of a single peptide-encapsulated Ag_n NC positioned between the monochromator slits [vertical white lines in (a) and (b)] excited at 514.5 nm, 30 W/cm^2. (d) PAMAM-encapsulated Ag_n dark-field and (e) Stokes-shifted emission image of the same field of view. (f) Emission spectrum of a dendrimer-encapsulated Ag NC. Dark-field scattering arises only from glass imperfections and is completely uncorrelated with emissive features.

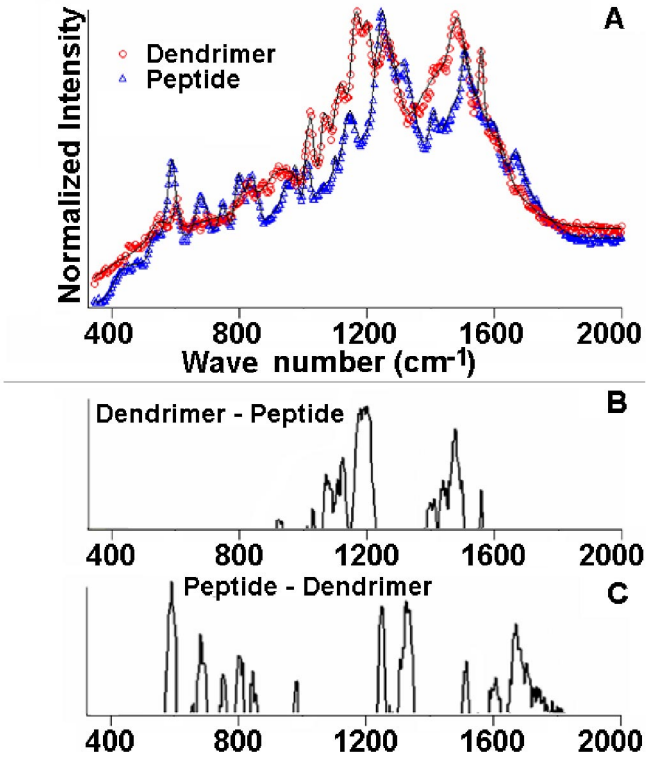

FIG. 2 (color online). (a) Summed Raman spectra from 100 PAMAM- (○) and 100 peptide-encapsulated (△) Ag_n NCs. Spectral subtractions remove the similar NC fluorescent background and yield characteristic (b) dendrimer and (c) peptide Raman lines when only positive peaks are retained for each subtraction order.

convoluted single-component lifetimes down to 7 ps. Lifetime measurements within 10-nm emission bandwidths yield instrument response function (IRF) limited emission detected shorter than 480 nm (consistent with Raman and the lack of Ag nanocluster fluorescence at these short wavelengths [15]), apparent decays of 11 ps between 480–500 nm, and single-component, ~30 ps decays beyond 500 nm. The slightly broadened time response just below 500 nm is consistent with the dominant instantaneous Raman emission close to the 445-nm excitation and a small amount of 30-ps Ag nanocluster fluorescence. Deconvolution of these very similar time components (strong 35 ps IRF-generating Raman and weak 30-ps fluorescence convoluted with the IRF) cannot resolve the two decays; only a very slightly broadened decay consistent with the postdeconvolution, apparent 11 ps emission, is observed in this spectral range. Emission longer than 500 nm produces deconvoluted single-component decays of 30 ps from the dominant broad fluorescent Ag NC background on which the shorter wavelength, sharp Raman lines appear.

The finite lifetime suggests that if Raman enhancement and the fluorescent background arise from excitation of an individual Ag NC, fluorescence antibunching should be observable. With sufficiently short pulse excitation, only one photon can be emitted per excitation pulse if each pulse is extremely short relative to the NC lifetime. Measured as arrival time histograms between photon pairs arriving on two avalanche photodiodes, such histograms should produce reduced coincidence counts at zero delay if the signal arises from a single quantum system [20]. When excited with ~6-ps pulses at 532 nm and collecting all Ag_n fluorescence and PAMAM Raman emission longer than 570 nm, a weak antibunching feature is observed with a high S/N ratio (Fig. 3, inset). As multiple Raman modes can be excited within each pulse and 6 ps is only a factor of 2–5 faster than either vibrational depopulation or Ag_n fluorescence, the coincidence counts at $\tau = 0$ will not reach zero. In order to decrease the probability of simultaneous 2-photon emission, doubled Ti:sapphire excitation at 445 nm (~200 fs) was used while collecting emission longer than 590 nm to shift beyond all Raman lines and any fluorescence from the optics. Under these conditions, antibunching from the small amount of Ag NC emission that remains is clearly observed (Fig. 3), but only after rejecting more than 90% of the total emission, severely limiting the contrast. The long wavelength portion of the NC emission exhibits a reduced intensity at zero interphoton arrival delay, thereby proving that emission is from a single NC. This confirms for the first time that Raman can be definitively observed from a single molecule system, and concurrently that individual Ag NCs enhance Raman scattering well above observable single molecule levels.

Surprisingly, the Raman transitions are so strong that even the anti-Stokes (AS) lines are readily observed on the single molecule level [Figs. 4(a) and 4(c)]. At 1/80th of the strength of the 1550 cm^{-1} Stokes-shifted line, these higher energy transitions are stronger than expected from a thermal distribution of scaffold excited vibrational state populations. As high-intensity conditions for potential optical pumping are not present in this work [21], the observed deviation from a thermal distribution and quadratic dependence on excitation intensity may result from preferential AS enhancement due to a recently reported metal-molecule charge transfer [22]. Exhibiting identical shifts to the Stokes-shifted transitions, these higher energy AS-

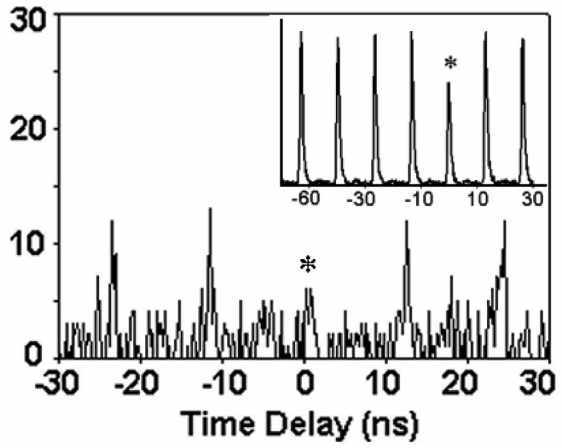

FIG. 3. Single PAMAM-encapsulated Ag_n coincidence counts (inset) with 6-ps, 532-nm excitation, collected longer than 570 nm, and (main) with 200-fs, 445-nm excitation, collected longer than 590 nm. Shorter excitation pulses and larger spectral shifts from the excitation frequency enable NC antibunching to be more clearly observed at zero delay (*). The reduced peak only at zero delay indicates a sub-Poissonian source, with greatly reduced coincidences signifying emission of approximately one photon at a time—proof of single molecule emission.

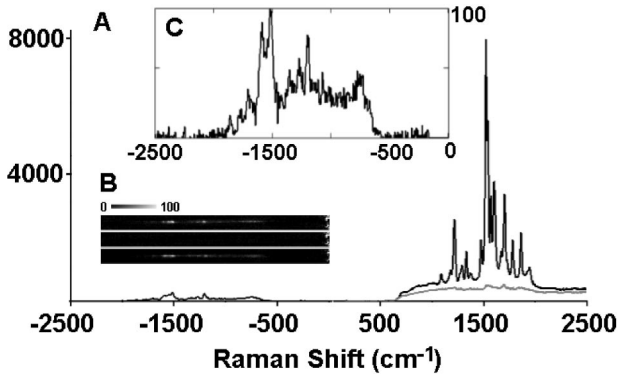

FIG. 4. (a) Stokes-shifted (right, positive shifts to lower energy) and anti-Stokes–shifted (left, negative shifts to higher energy) Raman spectra for an individual dendrimer-encapsulated Ag NC. AS-shifted frequencies match exactly with their Stokes counterparts. Lower (gray) Stokes-shifted spectrum shows fluorescence observed from the dendrimer-encapsulated NC when Raman scattering has blinked off. (b) With the same spectral axis as (a), three successive 10-s frames show intermittency of the AS emission. (c, inset) Expanded AS spectrum from (a).

Raman features also blink [Fig. 4(b)] and occur on top of a weak background of currently unknown origin. AS spectra are excited at the same 30 W/cm^2 intensities at 514.5 nm and are collected at 10-s exposures through short pass optics to image the higher energy emission. Stokes and AS emission from the exact same encapsulated NCs are measured by switching filters within the microscope filter turret during the same data set. This is the first observation of single molecule AS-Raman and should provide true background free windows for biological imaging by measuring emission at higher energy than the excitation [23]. With the AS signal being $\sim 1/80$th of the Stokes lines, AS-Raman transitions exhibit intensities comparable to standard single molecule fluorescence from the best organic dyes. As observed with the Stokes-shifted lines, the SM-AS of the peptide (not shown) and of the PAMAM are distinctly different and the frequencies of each match their respective Stokes-shifted counterparts. All Raman lines and fluorescent backgrounds are also observed when excited closer to resonance at 476 nm.

The observed total absorption cross sections are comparable to those observed for Ag NCs on roughened thin Ag and AgO films as well as those encapsulated in PAMAM dendrimers in solution ($\sigma = 10^{-14}$ cm^2) [14,15]. Accordingly, both the SM-Raman and Ag_n fluorescence likely stem from initial Ag nanocluster electronic excitation. Since the laser excitation is well overlapped with the electronic absorption of the silver NCs [24], a type of resonance or preresonance enhancement likely occurs, but without plasmon enhancement as our few-atom Ag NCs are too small to support such a collective electron oscillation. As metal NCs are highly polarizable [25–27] and exhibit giant resonances in their gas phase photofragmentation [28] and photoelectron-ejection spectra [29], it is possible that either a predissociative or photoelectron-ejection process is accessed in the excited state leading to significant transfer of charge to the scaffold and significant Franck-Condon overlap with the scaffold vibrational levels. While the scaffold stabilizes the Ag NC and prevents photodissociation characteristic of gas phase Ag_n [25–28], a large excited state charge separation most likely produces the large oscillator strength, fast radiative lifetime, and Raman-enhancing ability of these few-atom NCs. Consequently, while not well understood at this time, the Raman transitions seem to ''piggyback'' off the strong Ag NC optical transition to yield the strong SM-Raman signals.

Without an enhancing NP, observation of SM-Stokes- and AS-shifted Raman, together with antibunched emission offers new insights into the nature of SM-Raman. The extremely high oscillator strength of these sub-nm NCs presents new possibilities for use as Raman labels with various scaffolds giving single molecule sensitivity correlated with true chemical information.

The authors gratefully acknowledge the National Science Foundation (Grant No. BES0323453), National Institutes of Health (Grants No. R01 GM068732 and No. P20 GM072021), and Vasser Woolley, Dreyfus, and Sloan Foundation for support. L. P. C. acknowledges support from an NSF IGERT. Also appreciated are assistance from C. Hladik and Y.-L. Tzeng and an equipment loan from Toptica, Inc.

*Current address: Materials Division, NASA Glenn Research Center, Cleveland, OH 44135, USA.
†Current address: Department of Applied Physics and Physics, Stanford University, Stanford, CA 94305, USA.
‡Author to whom correspondence should be addressed. Electronic address: dickson@chemistry.gatech.edu

[1] S. M. Nie and S. R. Emory, Science **275**, 1102 (1997).
[2] K. Kneipp *et al.*, Phys. Rev. Lett. **78**, 1667 (1997).
[3] A. M. Michaels, M. Nirmal, and L. E. Brus, J. Am. Chem. Soc. **121**, 9932 (1999).
[4] P. Hildebrandt and M. Stockburger, J. Phys. Chem. **88**, 5935 (1984).
[5] M. Moskovits, J. Chem. Phys. **69**, 4159 (1978).
[6] K. Kneipp, L. T. Perelman, and H. Kneipp, Phys. Rev. B **63**, 193411 (2001).
[7] J. Jiang *et al.*, J. Phys. Chem. B **107**, 9964 (2003).
[8] A. M. Michaels, J. Jiang, and L. E. Brus, J. Phys. Chem. B **104**, 11 965 (2000).
[9] K. L. Kelly *et al.*, J. Phys. Chem. B **107**, 668 (2003).
[10] C. L. Haynes and R. P. Van Duyne, J. Phys. Chem. B **107**, 7426 (2003).
[11] P. C. Andersen, M. L. Jacobson, and K. L. Rowlen, J. Phys. Chem. B **108**, 2148 (2004).
[12] O. L. A. Monti, J. T. Fourkas, and D. J. Nesbitt, J. Phys. Chem. B **108**, 1604 (2004).
[13] S. Fedrigo, W. Harbich, and J. Buttet, J. Chem. Phys. **99**, 5712 (1993).
[14] L. A. Peyser *et al.*, Science **291**, 103 (2001).
[15] J. Zheng and R. M. Dickson, J. Am. Chem. Soc. **124**, 13 982 (2002).
[16] J. M. Slocik, J. T. Moore, and D. W. Wright, Nano Lett. **2**, 169 (2002).
[17] L. A. Peyser, T.-H. Lee, and R. M. Dickson, J. Phys. Chem. B **106**, 7725 (2002).
[18] J. Zheng *et al.*, J. Phys. Chem. B **106**, 1252 (2002).
[19] A. P. Davis, G. Ma, and H. C. Allen, Anal. Chim. Acta **496**, 117 (2002).
[20] P. Kumar *et al.*, J. Am. Chem. Soc. **126**, 3376 (2004).
[21] K. Kneipp *et al.*, Phys. Rev. Lett. **76**, 2444 (1996).
[22] A. G. Brolo, A. C. Sanderson, and A. P. Smith, Phys. Rev. B **69**, 045424 (2004).
[23] J.-X. Cheng *et al.*, Biophys. J. **83**, 502 (2002).
[24] V. Bonacic-Koutecky, V. Veyret, and R. Mitric, J. Chem. Phys. **115**, 10 450 (2001).
[25] J. Ho, K. Ervin, and W. C. Lineberger, J. Chem. Phys. **93**, 6987 (1990).
[26] U. Hild *et al.*, Phys. Rev. A **57**, 2786 (1998).
[27] V. Spasov *et al.*, J. Chem. Phys. **110**, 5208 (1999).
[28] J. Tiggesbaumker *et al.*, Chem. Phys. Lett. **190**, 42 (1992).
[29] A. Henglein, P. Mulvaney, and T. Linnert, Faraday Discuss. **92**, 31 (1991).